


Research Article

Levitation Stability and Hopf Bifurcation of EMS Maglev Trains

Junxiong Hu,^{1,2} Weihua Ma ¹, Xiaohao Chen,¹ and Shihui Luo¹

¹State Key Laboratory of Traction Power, Southwest Jiaotong University, Chengdu 610031, China

²Henan Engineering Research Center of Rail Transit Intelligent Security, Zhengzhou Railway Vocational & Technical College, Zhengzhou 451460, China

Correspondence should be addressed to Weihua Ma; mwh@swjtu.edu.cn

Received 28 July 2019; Accepted 28 February 2020; Published 7 April 2020

Academic Editor: Xiao-Qiao He

Copyright © 2020 Junxiong Hu et al. This is an open access article distributed under the Creative Commons Attribution License, which permits unrestricted use, distribution, and reproduction in any medium, provided the original work is properly cited.

This paper analyzed the mechanical characteristics of single electromagnet system and elastic track beam of EMS maglev train and established a five-dimensional dynamics model of single electromagnet-track beam coupled system with classical PD control strategy adopted for its levitation system. Then, based on the Hurwitz criterion and the high-dimensional Hopf bifurcation theory, the stability of the coupled system is analyzed; the existence of the Hopf bifurcation is discussed and the bifurcation direction and the stability of the periodic solution are determined with levitation control feedback coefficient k_p as the bifurcation parameter; and numerical simulation is conducted to verify the validity of the theoretical analysis results. The results show that the Hurwitz algebra criterion can directly determine the eigenvalues and symbols of the dynamics system to facilitate the analysis on the stability of the system and the Hopf bifurcation without the necessity of calculating the specific eigenvalues; supercritical Hopf bifurcation will occur under the given parameters, that is, when $k_p < k_{p_0}$, the real-time system is asymptotically stable, yet Hopf bifurcation occurs as k_p increases gradually beyond k_{p_0} , with the stability of the system lost and a stable limit cycle branched.

1. Introduction

Maglev train is a new type of rail transit vehicle that has gradually emerged in recent years. It uses electromagnets, permanent magnets, etc., to interact with the track to generate magnetic force and levitate the train and also uses linear motor for traction so that the contactless operation between the train and the track is realized. From the perspective of the principle of levitation, currently there are two typical and mature types of maglev trains: electromagnetic suspension (EMS) and electrodynamic suspension (EDS). EMS maglev train generates a magnetic field by energizing the electromagnet attached to the train, and the electromagnet and the track attract each other to levitate the train. The levitation gap is generally 8~12 mm, and form of the elevated bridge line is adopted. Due to the small levitation gap of the EMS maglev train and the nonlinear characteristics of the levitation system, there is a special coupled vibration problem between the train and the track beam, which may even lead to a levitation failure in severe cases [1]. This vibration problem is a high-dimensional and nonlinear

complex problem involving bridge structure vibration, vehicle vibration, and stability control of levitation system. To solve this technical problem, many experts and scholars have conducted studies from different angles in the aim of finding the couple mechanism and solving the problem once and for all to ensure the levitation stability of the train.

As early as 1986, Nagai noticed the nonlinear self-excited vibration of the track beam due to the neglect of the elastic deformation of the track beam during the design process of the controller and designed a control algorithm so that the vehicle can be stabilized in the elastic track beam and is insensitive to elastic conditions [2]. Cai et al. considered the interaction between the elastic track beam and the moving train, simplified the “vehicle-guideway” system to the “moving load-simple beam” system, and studied the different dynamics of the beam when the moving load was applied to single- and double-span beams [3]. Lee et al. have conducted a lot of research studies on the train-track beam coupled vibration behavior of the low-speed maglev in Korea and have obtained a series of research results [4–6]. Based on the analysis of the structural characteristics of the

EMS train system, Xie and Chang simulated and analyzed the effects of the damping of elastic track beam and acceleration feedback gain upon static levitation stability and dynamic characteristics [7]. Zhao and Zhai studied and analyzed the vertical dynamics behavior of German TR (Transrapid) high-speed maglev trains and China's self-developed low-speed maglev trains [8]. Ma et al. established test bench for electromechanical coupled vibration of single-levitation frame for medium- and low-speed maglev trains and carried out simulation analysis and experimental comparison of vehicle-guideway coupled vibration under different combinations of boundary conditions such as track beam support stiffness, levitation mass, and control algorithm [9].

The levitation control system of EMS maglev train is a typical nonlinear dynamic system, and the change of system parameters will generate new dynamics behavior and even undermine the stability of the system. Zhou and Zheng established the ordinary differential equations of the vehicle-track beam coupled dynamics with periodically variable coefficients. The Lyapunov characteristic index was used to determine the dynamic stability of the maglev system, and the possibility of chaotic phenomena in the system under the nonlinear conditions of the secondary suspension was studied [10]. Shi et al. analyzed the Hopf bifurcation of nonlinear magnetic levitation system based on PID controller and explained the reasons for the vibration of the system from the perspective of control parameters and the stability of periodic solution [11]. Wang et al. used the center manifold reduction method and Poincaré canonical method to study the Hopf bifurcation and resonance problems of the levitation system under positional delay and track beam disturbance [12, 13]. Li et al. established a single electromagnet-track beam model to study the mechanism of self-excited vibration caused by the transfer of vibration energy from levitation system to track beam and compared the stability of the system under different PD control parameters [14]. Zhao and Zhai numerically simulated the dynamic stability of a single electromagnet system, pointing out that the difference between the secondary suspension frequency, the track beam fundamental frequency, and the control system frequency should be as large as possible to avoid resonance between the single electromagnet and the track beam, which may lead to system instability [15]. Based on the similarity theory, Wang and Shen established a small-scale model of single-electromagnetic vehicle-track beam coupled system, derived the similarity relationship in the dynamic system, and analyzed the similarity characteristics of the small-scale model [16]. They also studied the optimal control method on the elastic track beam and established a test rig of small-scale single electromagnet-elastic track beam for verification [17]. Zhang et al. studied the stability of the time-delay levitation system and the Hopf bifurcation under the sliding mode control strategy [18, 19]. Based on the Hurwitz algebraic criterion, Wu and Fang analyzed the conditions for Hopf bifurcation to occur without considering the influence of the elasticity of the track beam [20]. Sun et al. analyzed the relationship between the control parameters and the Hopf bifurcation of the maglev

vehicle-guideway coupling system and designed a fuzzy adaptive controller to adjust the control parameters automatically to keep the closed-loop system away from the Hopf bifurcation point [21].

In this paper, analysis is conducted on the stability of the levitation system of the EMS maglev train on elastic track beam. The research object is a levitation control unit in the decentralized control point of the maglev train—a single electromagnet system. In the first part, a simplified dynamics model of “electromagnet-levitation control system-elastic track beam” is established; the second part discusses the equilibrium point of the canonical form of the model and its stability; the third part uses the control coefficient k_p as the bifurcation parameter, introduces the method of directly determining the Hopf bifurcation of the levitation control system by using the Hurwitz criterion, and further discusses the direction of Hopf bifurcation and the stability of bifurcation periodic solution by means of the high-dimensional Hopf bifurcation theory. The fourth part uses the numerical simulation method to verify the theoretical analysis results.

2. Modeling

EMS maglev train adopts electromagnetic attraction type of levitation, that is, it relies on the attraction between the vehicle electromagnet and the F -shaped ferromagnetic track to achieve levitation. The active control method must be adopted to ensure the stable levitation of the train. At present, EMS maglev trains mostly adopt the technical scheme of multipoint decentralized control. The electromagnet controlled by one set of levitation controller is a single-magnet levitation system, many of which compose the levitation system of EMS maglev train. The simplified single electromagnet system is shown in Figure 1.

Under the assumption of neglecting the leakage of the electromagnet winding and the magnetic resistance of the electromagnet core and the guideway, the following equations for the system model shown in (1) can be obtained:

$$\left\{ \begin{array}{l} \text{electromagnet force equation: } F = k \left(\frac{I}{\delta} \right)^2, \quad k = \frac{\mu_0 N^2 A_m}{4}, \\ \text{dynamic equation: } m\ddot{z} = mg - F, \\ \text{electrical equation: } u = RI + \frac{2k}{\delta} \dot{I} - \frac{2kI}{\delta^2} \dot{\delta}, \end{array} \right. \quad (1)$$

where F is levitation force, μ_0 is vacuum permeability, N is the turns of electromagnet coil, A_m is the area of electromagnet pole, m is sum of a single electromagnet's own weight and load weight, I is exciting current, R is electromagnet resistance, u is the voltage at electromagnet end, z is absolute gap between the electromagnet and the rigid track, and δ is actual levitation gap of the electromagnet.

The voltage feedback control adopts the classic PD control. k_p and k_d are the gap offset and the gap differential feedback coefficients, respectively. Therefore,

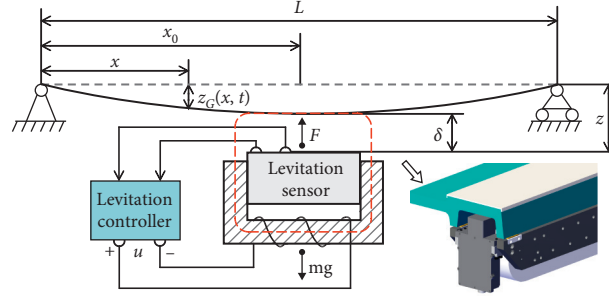


FIGURE 1: Simplified single electromagnet-track beam coupled model.

$$u_c = u_0 + k_p (\delta - \delta_0) + k_d \dot{\delta}, \quad (2)$$

where u_0 is the initial voltage at equilibrium position and δ_0 is the desired levitation gap.

Assume that the track beam is a simply supported and evenly elastic beam with equal cross section; then, the following can be obtained by the Bernoulli-Euler beam equation:

$$EI_g \frac{\partial^4 z_G}{\partial x^4} + \rho A_g \frac{\partial^2 z_G}{\partial t^2} + C \frac{\partial z_G}{\partial t} = F(x, t), \quad (3)$$

where E is Young's modulus of elasticity, I_g is beam section inertia, C is equivalent damping coefficient of the beam, ρ is beam density, A_g is area of beam section, and $F(x, t)$ is levitation load intensity acting on the beam.

Using the modal superposition method, the displacement of the beam in equation (3) can be expressed as the linear superposition of a regular mode function $\varphi_i(x)$ and a generalized coordinate $q_i(t)$:

$$z_G(x, t) = \sum_{i=1}^n \varphi_i(x) \cdot q_i(t). \quad (4)$$

Integrating equation (4) into equation (3) gives the vibration equation corresponding to the i^{th} -order mode of the beam

$$\ddot{q}_i(t) + 2\eta_i \omega_i \dot{q}_i(t) + \omega_i^2 q_i(t) = Q_i, \quad (5)$$

where ω_i is the i^{th} -order natural frequency of the beam, η_i is the i^{th} -order damping ratio of the beam, and Q_i is the i^{th} -order generalized force.

For the simply supported single-span beam with the length of L in Figure 1, the natural frequency ω_i and the regular mode function $\varphi_i(x)$ of the beam are, respectively, given by

$$\omega_i = \left(\frac{i\pi}{L}\right)^2 \sqrt{\frac{EI}{\rho A_g}}, \quad (6)$$

$$\varphi_i(x) = \sqrt{\frac{2}{m_G}} \cdot \sin\left(\frac{i\pi x}{L}\right), \quad 0 \leq x \leq L. \quad (7)$$

While conducting studies on the coupled vibration of the EMS maglev train, Shi et al. found that the high-order vibration mode can only occur with exceptionally high energy

excitation [11]. From the latest test results from Li and others on the Changsha maglev line, it can be seen that for a definite track beam structure, the vibration frequency corresponding to the maximum amplitude of track beam with maglev train running on its upper part is distributed within a range, wherein the first-order frequency of the track beam has the greatest impact [22]. Therefore, only the influence of the first-order bending mode of the track beam is taken into account in the analysis of this paper. Since the length of the electromagnet is much smaller than the span of the track beam, the electromagnetic force F can be considered as a concentrated load acting at position x_0 on the track beam when seeking the limit through the generalized force expression. The first-order vibration equation of the generalized coordinates of the track can be rewritten as

$$\ddot{q}_1 + 2\eta_1 \omega_1 \dot{q}_1 = \varnothing_1 F, \quad (8)$$

where $\varnothing_1 = \sqrt{2/m_G} \cdot \sin(\pi x_0/L)$, $\omega_1 = (\pi^2/L^2) \sqrt{(EI_g/\rho A_g)}$, and $2\eta_1 \omega_1 = (C/\rho)$.

Introducing the deformation of the track beam $z_G = \varnothing_1 q_1$ into the vibration equation (8), where \varnothing_1 is a constant, we can obtain

$$\ddot{z}_G + 2\eta_1 \omega_1 \dot{z}_G + \omega_1^2 z_G = \varnothing_1^2 F. \quad (9)$$

In the midspan position where the amplitude of the simply supported beam is the largest, we have $x_0 = (L/2)$, and then $\varnothing_1 = \sqrt{(2/m_G)}$.

Therefore, the coupled system model under the influence of the first-order vibration mode of the track can be defined by

$$\begin{cases} m\ddot{z} = mg - F, \\ \dot{I} = \frac{I}{\delta} \dot{\delta} + \frac{\delta}{2k} \left[u_0 + k_p (\delta - \delta_0) + k_d \dot{\delta} \right] - \frac{RI}{2k} \delta, \\ \ddot{z}_G + 2\eta_1 \omega_1 \dot{z}_G + \omega_1^2 z_G = \varnothing_1^2 F. \end{cases} \quad (10)$$

3. Equilibrium Points and Their Stability

Let $\mathbf{X} = [x_1 \ x_2 \ x_3 \ x_4 \ x_5]^T = [z \ \dot{z} \ \delta \ \dot{\delta} \ I]^T$ and levitation gap $\delta = z - z_G$; then, the canonical form of the coupled system model (10) is determined as follows:

$$\left\{ \begin{array}{l} \dot{x}_1 = x_2, \\ \dot{x}_2 = g - \frac{k}{m} \left(\frac{x_5}{x_3} \right)^2, \\ \dot{x}_3 = x_4, \\ \dot{x}_4 = g - \frac{k}{m} \left(\frac{x_5}{x_3} \right)^2 - \left[-2\eta_1 \omega_1 (x_2 - x_4) - \omega_1^2 (x_1 - x_3) + \varnothing_1^2 k \left(\frac{x_5}{x_3} \right)^2 \right], \\ \dot{x}_5 = \frac{x_5}{x_3} x_4 + \frac{x_3}{2k} [u_0 + k_p (x_3 - \delta_0) + k_d x_4] - \frac{R}{2k} x_3 x_5. \end{array} \right. \quad (11)$$

It can be seen from equations (11) that the EMS maglev train-track beam coupled system is a typical nonlinear system, which also brings certain difficulties for solving. The core work of this paper is to study the local stability of the coupled system at the equilibrium point and the Hopf bifurcation of the control parameters.

Let $\dot{\mathbf{X}} = [\dot{x}_1 \ \dot{x}_2 \ \dot{x}_3 \ \dot{x}_4 \ \dot{x}_5]^T = 0$ and we have $mg = k(I_0/\delta_0)^2$ at the desired levitation gap and $u_0 = I_0 R$; then, the equilibrium point can be given by

$$\mathbf{X}_0 = [x_1^0 \ x_2^0 \ x_3^0 \ x_4^0 \ x_5^0]^T = \left[\delta_0 + \frac{mg\varnothing_1^2}{\omega_1^2} \ 0 \ \delta_0 \ 0 \ \delta_0 \sqrt{\frac{mg}{k}} \right]^T. \quad (12)$$

Shift the equilibrium point \mathbf{X}_0 of the system (11) to the original point $o(0 \ 0 \ 0 \ 0 \ 0)$ through the transformation $\bar{\mathbf{X}} = \mathbf{X} + \mathbf{X}_0$, and the new system (13) is expressed as

$$\left\{ \begin{array}{l} \bar{x}_1 = \bar{x}_2, \\ \bar{x}_2 = g - \frac{k}{m} \left(\frac{\bar{x}_5 + x_5^0}{\bar{x}_3 + x_3^0} \right)^2, \\ \bar{x}_3 = \bar{x}_4, \\ \bar{x}_4 = g - \frac{k}{m} \left(\frac{\bar{x}_5 + x_5^0}{\bar{x}_3 + x_3^0} \right)^2 - \left[-2\eta_1 \omega_1 (\bar{x}_2 - \bar{x}_4) - \omega_1^2 \left(\bar{x}_1 + \frac{mg\varnothing_1^2}{\omega_1^2} - \bar{x}_3 \right) + \varnothing_1^2 k \left(\frac{\bar{x}_5 + x_5^0}{\bar{x}_3 + x_3^0} \right)^2 \right], \\ \bar{x}_5 = \left(\frac{\bar{x}_5 + x_5^0}{\bar{x}_3 + x_3^0} \right) \bar{x}_4 + \frac{\bar{x}_3 + x_3^0}{2k} (u_0 + k_p \bar{x}_3 + k_d \bar{x}_4) - \frac{R}{2k} (\bar{x}_3 + x_3^0) (\bar{x}_5 + x_5^0). \end{array} \right. \quad (13)$$

The Jacobian matrix of system (13) at the original point $o(0 \ 0 \ 0 \ 0 \ 0)$ is given by

$$\mathbf{A} = \begin{bmatrix} 0 & 1 & 0 & 0 & 0 \\ 0 & 0 & \frac{2g}{\delta_0} & 0 & -\frac{2k}{m\delta_0} \sqrt{\frac{mg}{k}} \\ 0 & 0 & 0 & 1 & 0 \\ \omega_1^2 & 2\eta_1\omega_1 & \frac{2g(1+m\varnothing_1^2)}{\delta_0} - \omega_1^2 & -2\eta_1\omega_1 & -\frac{2k(1+m\varnothing_1^2)}{m\delta_0} \sqrt{\frac{mg}{k}} \\ 0 & 0 & \frac{k_p\delta_0}{2k} & \frac{k_d\delta_0}{2k} + \sqrt{\frac{mg}{k}} & -\frac{R\delta_0}{2k} \end{bmatrix}. \tag{14}$$

The corresponding characteristic equation is written as

$$f(\lambda) = \lambda^5 + a_1\lambda^4 + a_2\lambda^3 + a_3\lambda^2 + a_4\lambda + a_5. \tag{15}$$

Model parameters are shown in Table 1.

Substituting the parameters, the coefficients of characteristic equation (15) can be obtained:

$$\begin{cases} a_1 = 5.147, \\ a_2 = 4.154k_d + 3600.589, \\ a_3 = 11.131k_d + 4.154k_p + 2563.807, \\ a_4 = 14518.156k_d + 11.131k_p - 16159.558, \\ a_5 = 14518.156k_p - 21077684.888. \end{cases} \tag{16}$$

According to Liénard–Chipart criterion, the necessary and sufficient conditions for all eigenvalues of the characteristic equation (15) to have a negative real part are that the characteristic equation coefficients are all greater than 0, and half of the Hurwitz determinant is greater than 0, namely,

$$a_i > 0, \quad (i = 1 \sim 5),$$

$$\Delta_2 = \begin{vmatrix} a_1 & 1 \\ a_3 & a_2 \end{vmatrix} = a_1a_2 - a_3 > 0,$$

$$\Delta_4 = \begin{vmatrix} a_1 & 1 & 0 & 0 \\ a_3 & a_2 & a_1 & 1 \\ a_5 & a_4 & a_3 & a_2 \\ 0 & 0 & a_5 & a_4 \end{vmatrix}$$

$$= -a_1^2a_4^2 - a_1a_2^2a_5 + a_1a_2a_3a_4 + 2a_1a_4a_5 + a_2a_3a_5 - a_3^2a_4 - a_5^2 > 0. \tag{17}$$

Therefore, the levitation control feedback coefficient k_p and k_d when the system is stable can be obtained, and the value range is shown in Figure 2.

4. Existence and Direction of Hopf Bifurcation

4.1. Existence of Hopf Bifurcation. For the classical Hopf bifurcation evaluation method, it is necessary to solve the eigenvalues of the Jacobian matrix whenever each parameter changes and judge whether the real part is zero. For the five-

order coupled vibration model to be studied in this paper, the calculation is cumbersome and not conducive to the development of research work. Thus, the Hopf bifurcation of parameter k_p is taken as an example. The algebraic criterion and calculation method of Hopf bifurcation occurring when the equilibrium point loses stability proposed in reference [23] are adopted, and the existence of the Hopf bifurcation point is directly determined based on the Hurwitz algebraic criterion, with three theorems first introduced as follows.

Theorem 1. *The necessary and sufficient conditions for the characteristic equation (15) to have a pair of pure imaginary eigenvalue and the remaining $n - 2$ eigenvalues to have negative real parts are*

$$a_i > 0, \quad (i = 1, 2, \dots, n), \Delta_i > 0, \quad (i = n - 3, n - 5, \dots), \Delta_{n-1} = 0, \tag{18}$$

where Δ_i is the Hurwitz determinant of the characteristic equation (15).

Theorem 2. *If the Hurwitz determinant of the characteristic equation (15) satisfies*

$$a_i > 0, \quad (i = 1, 2, \dots, n), \Delta_i > 0, \quad (i = n - 3, n - 5, \dots), \Delta_{n-1} = 0, \tag{19}$$

then the characteristic equation (15) has a pair of pure imaginary eigenvalues $\pm \omega i$, and the remaining $n - 2$ eigenvalues have negative real parts, and

$$\omega^2 = \frac{\Delta_{n-3}}{\Delta_{n-2}} a_n. \tag{20}$$

Theorem 3. *If the eigenvalues of characteristic equation (15) at $\mu = \mu_0$ all have negative real parts, and the Hurwitz determinant satisfies the following conditions:*

$$(i) \Delta_{n-3}(\mu_c) > 0$$

where $\mu_c = \min\{|\mu - \mu_0| : \Delta_{n-1}(\mu) = 0\}$, then the characteristic equation (15) has a pair of pure imaginary eigenvalues at $\mu = \mu_c$, and the other eigenvalues all have negative real parts. Let \mathbf{U} and \mathbf{V} be the left and right eigenvectors of the matrix $\mathbf{A}(\mu_c)$ corresponding to the eigenvalues $i\omega_c$, respectively, $\mathbf{UV} = 1$.

TABLE 1: Model parameter values.

μ_0	M (kg)	R (Ω)	N	δ_0 (m)
$4\pi e - 7$	750	0.48	320	0.008
A_m (m^2)	m_G (kg)	ω_1 (rad/s)	η_1	
0.025	$5e4$	60	0.023	

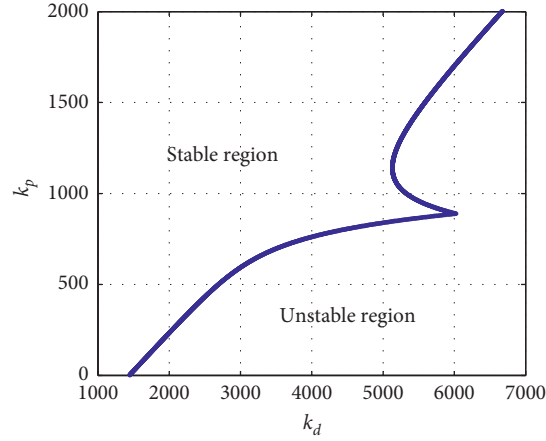


FIGURE 2: Relationship between system stability region and levitation control feedback coefficients.

(ii) $Re(\mathbf{UBV}) \neq 0$, where $\mathbf{B} = (d\mathbf{A}(\mu)/d\mu)|_{\mu=\mu_c}$.

Then, the Hopf bifurcation occurs at $\mu = \mu_c$, namely, there is periodic motion in the system near the parameters $\mu = \mu_c$.

Applying the aforementioned theorems to the problem in this paper, according to Theorem 1, the characteristic equation (15) has a pair of pure imaginary eigenvalues, and the remaining $n-2$ eigenvalues have negative real parts; then, we can obtain

$$\begin{aligned}
 & a_i > 0, \quad (i = 1, 2, \dots, n), \\
 & \Delta_2 = \begin{vmatrix} a_1 & 1 \\ a_3 & a_2 \end{vmatrix} = 10.250k_d - 4.154k_p + 16000.476 > 0, \\
 & \Delta_4 = \begin{vmatrix} a_1 & 1 & 0 & 0 \\ a_3 & a_2 & a_1 & 1 \\ a_5 & a_4 & a_3 & a_2 \\ 0 & 0 & a_5 & a_4 \end{vmatrix} \\
 & = 1.656e6k_d^3 - 192k_p^3 - 6.7e5k_d^2k_p - 40.69k_dk_p^2 \\
 & \quad - 1.722e9k_d^2 + 9.281e6k_p^2 + 1.109e9k_dk_p \\
 & \quad - 3.655e11k_d - 5.468e11k_p + 7.749e14 = 0.
 \end{aligned} \tag{21}$$

The range of control parameter when the characteristic equation (15) has a pair of pure imaginary eigenvalues and the remaining $n-2$ eigenvalues all have negative real parts is

$$1451.8 < k_p < 2.468k_d + 3851.824. \tag{22}$$

According to Theorem 2, let $k_d = 100$, and discuss the bifurcation parameter k_p . Get the critical value $k_{p_0} = 1690.681$ according to the equation $\Delta_4 = 0$ and substitute it in other parameter expressions. The calculation results are shown in Table 2.

It can be seen that $a_i > 0$ and $\Delta_2 > 0$ hold. Directly calculating the pair of pure imaginary eigenvalues of characteristic equation (15) of the system, we have $\omega_0^2 = (\Delta_2/\Delta_3)a_5 = 401.766$, and thus $\lambda_{1,2}(k_{p_0}) = \pm \omega_0 i = \pm 20.044i$.

According to Theorem 3, substitute the obtained pure imaginary eigenvalues into the system equation, and we can obtain left and right eigenvectors corresponding to $\lambda_1(k_{p_0}) = \pm \omega_0 i = \pm 20.044i$, satisfying $\mathbf{UV} = 1$:

$$\begin{aligned}
 \mathbf{U} &= [-1.973e3 - 33.863i, 0.177 + 98.472i, 1.246e4 + 1.427e3i, -0.189 - 10.987i, -3.476 - 0.415i], \\
 \mathbf{V} &= [-2.850e-4 + 1.601e-8i, -3.209e-7 - 5.712e-3i, -2.839e-4 - 2.623e-9i, 5.255e-8 - 5.691e-3i, -1]^T.
 \end{aligned} \tag{23}$$

TABLE 2: Calculation results when $k_d = 100$ and $k_{p_0} = 1690.681$.

a_2	a_3	a_4	a_5	Δ_2	Δ_3	Δ_2/Δ_3
4.022e3	1.070e4	1.455e6	3.468e6	1.000e4	8.634e7	1.159e-4

Let $\mathbf{B} = (d\mathbf{A}(k_{p_0}))/dk_{p_0} = \begin{bmatrix} 0 & 0 & 0 & 0 & 0 \\ 0 & 0 & 0 & 0 & 0 \\ 0 & 0 & 0 & 0 & 0 \\ 0 & 0 & 0 & 0 & 0 \\ 0 & 0 & 4.974 & 0 & 0 \end{bmatrix}$, and we have $\mathbf{UBV} = 0.0049 + 0.0006i$.

Therefore, there is $\text{Re}(\mathbf{UBV}) = 0.0049 \neq 0$, which satisfies the transversal condition. Then, when it is set that $k_d = 100$, $k_{p_0} = 1690.681$ is a Hopf bifurcation point of the system.

4.2. Direction and Stability of Hopf Bifurcating Periodic Solutions. Hassard et al. used the center manifold theory and the normal form approach to derive the formula for determining the Hopf bifurcation direction, periodic solution stability, and periodic variation of high-dimensional dynamic systems [24, 25] and further analyze the stability of periodic solutions near the aforementioned control parameters k_{p_0} and Hopf bifurcation direction. Suppose there

is a transformation matrix \mathbf{P} that transforms the system Jacobian matrix $\mathbf{A}(k_{p_0})$ into the following Jordan standard form:

$$\mathbf{P}^{-1}\mathbf{A}(k_{p_0})\mathbf{P} = \begin{bmatrix} \begin{pmatrix} 0 & -\omega_0 \\ \omega_0 & 0 \end{pmatrix} & 0 \\ 0 & \mathbf{D} \end{bmatrix} = \mathbf{J}(k_{p_0}), \quad (24)$$

where the matrix $\mathbf{P} = [\text{Re}(\mathbf{v}_1) \text{Im}(\mathbf{v}_1) \mathbf{v}_3 \mathbf{v}_4 \mathbf{v}_5]$, in which \mathbf{v}_1 is the eigenvector corresponding to complex eigenvalue $\lambda_1(k_{p_0}) = \omega_0 i = 20.044i$ and $\text{Re}(\mathbf{v}_1)$ is the real part of \mathbf{v}_1 while $\text{Im}(\mathbf{v}_1)$ is the imaginary part of \mathbf{v}_1 ; \mathbf{D} is the diagonal matrix composed of real eigenvalues $\lambda_3(k_{p_0})$, $\lambda_4(k_{p_0})$, and $\lambda_5(k_{p_0})$; \mathbf{v}_3 , \mathbf{v}_4 , and \mathbf{v}_5 are the eigenvectors of the corresponding eigenvalues; and \mathbf{P} and \mathbf{P}^{-1} are given by

$$\mathbf{P} = \begin{bmatrix} -2.850e-4 & -1.601e-8 & -3.165e-5 + 1.454e-6i & -3.165e-5 - 1.454e-6i & -3.314e-4 \\ -3.209e-7 & 5.712e-3 & -4.373e-5 - 1.904e-3i & -4.373e-5 + 1.904e-3i & 7.915e-4 \\ -2.839e-4 & 2.623e-9 & -2.839e-4 - 8.870e-10i & -2.839e-4 + 8.870e-10i & -3.314e-4 \\ 5.255e-8 & 5.691e-3 & 3.912e-4 - 1.706e-2i & 3.912e-4 + 1.706e-2i & 7.916e-4 \\ -1 & 0 & -1 & & \end{bmatrix}, \quad (25)$$

$$\mathbf{P}^{-1} = \begin{bmatrix} -3.947e3 & 0.353 & 2.493e4 & -0.377 & -6.953 \\ 67.726 & 1.969e2 & 2.853e3 & -21.974 & -0.830 \\ 1.974e3 - 56.591i & -0.181 - 32.843i & -1.928e3 + 57.127i & 0.189 + 32.967i & -0.015 - 7.937e-5i \\ 1.974e3 + 56.591i & -0.181 + 32.843i & -1.928e3 - 57.127i & 0.189 - 32.967i & -0.015 + 7.937e-5i \\ -2.312e-2 & 9.660e-3 & -2.107e4 & 1.534e-5 & 5.983 \end{bmatrix}.$$

By substituting $\mathbf{Y} = \mathbf{P}^{-1}\bar{\mathbf{X}}$, the original system $\dot{\bar{\mathbf{X}}} = f(\bar{\mathbf{X}}, k_{p_0})$ is transformed into standardized form $\dot{\mathbf{Y}} = \mathbf{P}^{-1}f(\mathbf{PY}, k_{p_0})$, which can be expressed as

$$\begin{cases} \dot{y}_1 = -20.044y_2 + F_1(y_1, y_2, y_3, y_4, y_5), \\ \dot{y}_2 = 20.044y_1 + F_2(y_1, y_2, y_3, y_4, y_5), \\ \dot{y}_3 = (-1.379 + 60.098i)y_3 + F_3(y_1, y_2, y_3, y_4, y_5), \\ \dot{y}_4 = (-1.379 - 60.098i)y_3 + F_4(y_1, y_2, y_3, y_4, y_5), \\ \dot{y}_5 = -2.389y_5 + F_5(y_1, y_2, y_3, y_4, y_5). \end{cases} \quad (26)$$

At this time, the equilibrium point Y_0 of the new system (26) is the original point, $J(k_{p_0})$ is the Jacobian matrix of

system (26), and $F_i(y_1, y_2, y_3, y_4, y_5)$ is a high-order term. Then, the following values are obtained:

$$\begin{aligned}
 g_{20} &= \frac{1}{4} \left[\frac{\partial^2 F_1}{\partial y_1^2} - \frac{\partial^2 F_1}{\partial y_2^2} + 2 \frac{\partial^2 F_2}{\partial y_1 \partial y_2} + i \left(\frac{\partial^2 F_2}{\partial y_1^2} - \frac{\partial^2 F_2}{\partial y_2^2} - 2 \frac{\partial^2 F_2}{\partial y_1 \partial y_2} \right) \right], \\
 g_{11} &= \frac{1}{4} \left[\frac{\partial^2 F_1}{\partial y_1^2} + \frac{\partial^2 F_2}{\partial y_2^2} + i \left(\frac{\partial^2 F_2}{\partial y_1^2} + \frac{\partial^2 F_2}{\partial y_2^2} \right) \right], \\
 g_{02} &= \frac{1}{4} \left[\frac{\partial^2 F_1}{\partial y_1^2} - \frac{\partial^2 F_1}{\partial y_2^2} - 2 \frac{\partial^2 F_2}{\partial y_1 \partial y_2} + i \left(\frac{\partial^2 F_2}{\partial y_1^2} - \frac{\partial^2 F_2}{\partial y_2^2} + 2 \frac{\partial^2 F_2}{\partial y_1 \partial y_2} \right) \right], \\
 G_{21} &= \frac{1}{8} \left[\frac{\partial^3 F_1}{\partial y_1^3} + \frac{\partial^3 F_1}{\partial y_1 \partial y_2^2} + \frac{\partial^3 F_2}{\partial y_1^2 \partial y_2} + \frac{\partial^3 F_2}{\partial y_2^3} + i \left(\frac{\partial^3 F_2}{\partial y_1^3} + \frac{\partial^3 F_2}{\partial y_1 \partial y_2^2} - \frac{\partial^3 F_1}{\partial y_1^2 \partial y_2} - \frac{\partial^3 F_1}{\partial y_2^3} \right) \right], \\
 G_{110}^{k-2} &= \frac{1}{2} \left[\frac{\partial^2 F_1}{\partial y_1 \partial y_k} + \frac{\partial^2 F_2}{\partial y_2 \partial y_k} + i \left(\frac{\partial^2 F_2}{\partial y_1 \partial y_k} - \frac{\partial^2 F_1}{\partial y_2 \partial y_k} \right) \right]_{k=3,4,5} \\
 G_{101}^{k-2} &= \frac{1}{2} \left[\frac{\partial^2 F_1}{\partial y_1 \partial y_k} - \frac{\partial^2 F_2}{\partial y_2 \partial y_k} + i \left(\frac{\partial^2 F_2}{\partial y_1 \partial y_k} + \frac{\partial^2 F_1}{\partial y_2 \partial y_k} \right) \right]_{k=3,4,5}, \\
 w_{11}^{k-2} &= -\frac{1}{4\lambda_k} \left(\frac{\partial^2 F_k}{\partial y_1^2} + \frac{\partial^2 F_k}{\partial y_2^2} \right)_{k=3,4,5}, \\
 w_{20}^{k-2} &= \frac{1}{4(2\omega_0 i - \lambda_k)} \left(\frac{\partial^2 F_k}{\partial y_1^2} - \frac{\partial^2 F_k}{\partial y_2^2} - 2i \frac{\partial^2 F_k}{\partial y_1 \partial y_2} \right)_{k=3,4,5}, \\
 g_{21} &= G_{21} + \sum_{k=3}^5 (2G_{110}^{k-2} w_{11}^{k-2} + G_{101}^{k-2} w_{20}^{k-2}).
 \end{aligned} \tag{27}$$

Based on the above calculated values, let

$$\begin{aligned}
 C_1(0) &= \frac{i}{2\omega_0} \left(g_{20}g_{21} - 2|g_{11}|^2 - \frac{1}{3}|g_{02}|^2 \right) + \frac{1}{2}g_{21}, \\
 \mu_2 &= \frac{\text{Re}C_1(0)}{\alpha'(0)}, \\
 \tau_2 &= -\frac{\text{Im}C_1(0) + \mu_2\omega'(0)}{\omega_0}, \\
 \beta_2 &= 2\text{Re}C_1(0),
 \end{aligned} \tag{28}$$

where $\alpha'(0) = \text{Re}[\lambda'(k_p)|_{k_p=k_{p_0}}]$ and $\omega'(0) = \text{Im}[\lambda'(k_p)|_{k_p=k_{p_0}}]$.

Theorem 4. When the bifurcation parameter k_p of system (13) is increased beyond the critical value k_{p_0} , the Hopf bifurcation occurs at the equilibrium point $o(0 \ 0 \ 0 \ 0 \ 0)$, and the following characteristics exist:

(a) When $\mu_2 > 0$ ($\mu_2 < 0$), the Hopf bifurcation is a supercritical (subcritical) bifurcation, and a bifurcation periodic solution for $k_p > k_{p_0}$ ($k_p < k_{p_0}$) exists

(b) When $\beta_2 < 0$ ($\beta_2 > 0$), the bifurcation periodic solution is asymptotically stable (unstable)
 (c) When $\tau_2 > 0$ ($\tau_2 < 0$), the period of the periodic solution increases (decreases)

Substitute the system parameters to discuss the bifurcation direction when $k_d = 100$ and $k_{p_0} = 1690.681$. The calculation results of the above values are shown in Table 3.

Substituting the values yields $\mu_2 = 15.510 > 0$, $\beta_2 = -0.152 < 0$, and $\tau_2 = 6.682e - 4 > 0$.

It is known from $\mu_2 > 0$ that the Hopf bifurcation of system (13) at k_{p_0} is a supercritical bifurcation, that is, when $k_p < k_{p_0}$, the equilibrium point of the dynamical system is stable, yet Hopf bifurcation occurs as k_p is gradually increased to k_{p_0} . $\beta_2 < 0$ indicates that the periodic solution of the system bifurcation is a stable limit cycle, and the period of the periodic solution increases as the bifurcation parameter k_p increases because $\tau_2 > 0$.

5. Numerical Simulation

In this part, numerical simulation is used to verify the results of the above theoretical analysis. The dynamic characteristics of the system when $k_d = 100$ and $k_{p_0} = 1690.681$ are

TABLE 3: Calculation results of the relevant values in the bifurcation direction.

g_{20}	$0.696-4.17e-2i$	G_{110}^3	1.171	w_{11}^3	$-7.41e-2$
g_{11}	0.655	G_{101}^1	$0.945-1.172i$	w_{20}^1	$-1.369e-4+1.054e-4i$
g_{02}	$0.613+4.17e-2i$	G_{101}^2	$0.945+1.172i$	w_{20}^2	$-1.255e-5-8.619e-6i$
G_{21}	$2.27e-2$	G_{101}^3	1.184	w_{20}^3	$-3e-4+7.3e-3i$
G_{110}^1	$1.727-1.172i$	w_{11}^1	$-2.304e-5+7.558e-6i$	g_{21}	$-0.151+8.9e-3i$
G_{110}^2	$1.727+1.172i$	w_{11}^2	$-2.304e-5-7.558e-6i$	$C_1(0)$	$-0.076-2.27e-2i$

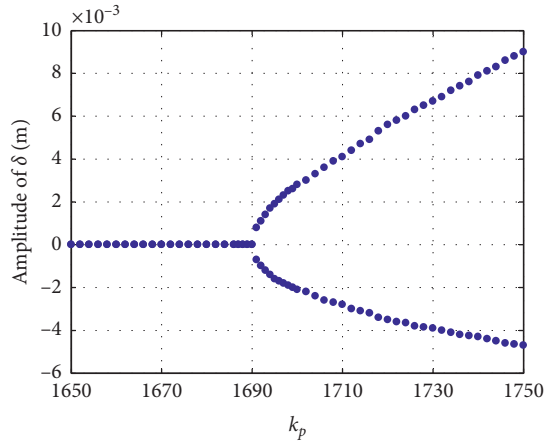


FIGURE 3: Local Hopf bifurcation diagram of system.

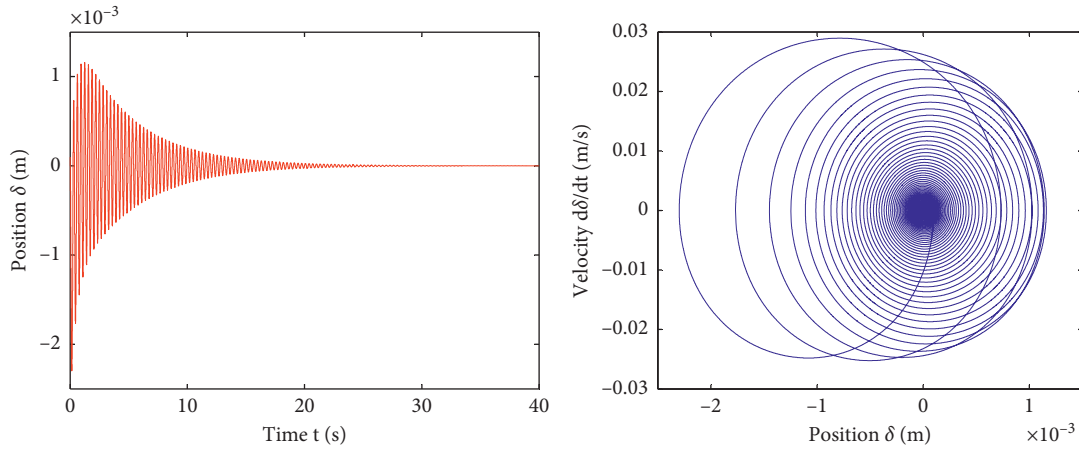


FIGURE 4: The response time domain and phase diagram when $k_p = 1650$.

analyzed through simulation, while other system parameters in Table 1 remain unchanged.

Give the system a small external disturbance, and the local Hopf bifurcation diagram of system (13) with k_p as the bifurcation parameter is shown in Figure 3. It can be seen that the system has a supercritical Hopf bifurcation, that is, the system equilibrium point is in a stable state when $k_p < k_{p_0}$ and Hopf bifurcation occurs when k_p is increased to k_{p_0} , while a stable limit cycle appears when $k_p > k_{p_0}$.

Figures 4–7 show the time history curves and phase before and after the bifurcation occurs when k_p takes

different values. It can be seen from the figure that the equilibrium point of the system is stable when $k_p < k_{p_0}$, yet the stability of the system equilibrium point is lost and a set of stable limit cycles is branched when k_p is increased beyond k_{p_0} .

It can also be seen from Figures 6 and 7 that each periodic solution is stable because $\beta_2 < 0$, and $\tau_2 > 0$ indicates that the period of the periodic solution increases as the bifurcation parameter k_p increases so that the period of the periodic solution when $k_p = 1800$ is greater than that when $k_p = 1700$.

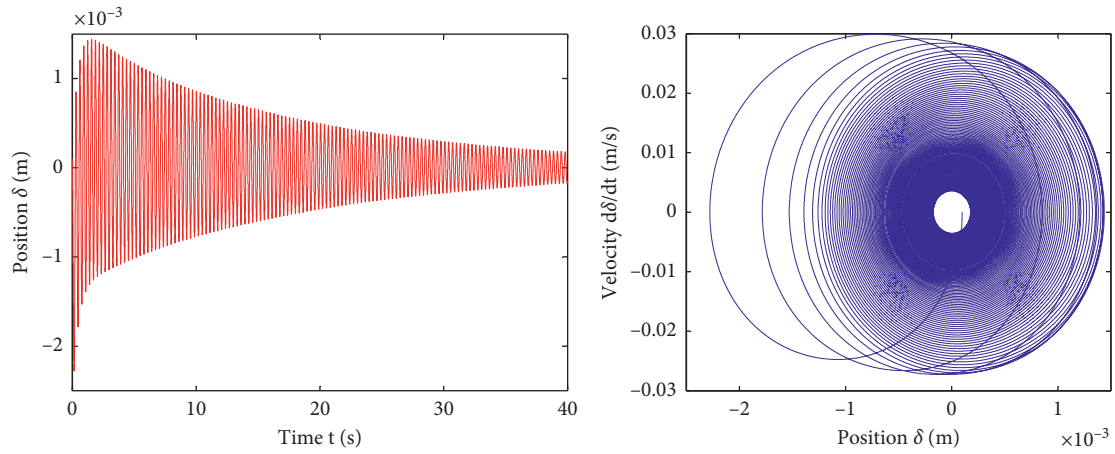


FIGURE 5: The response time domain and phase diagram when $k_p = 1680$.

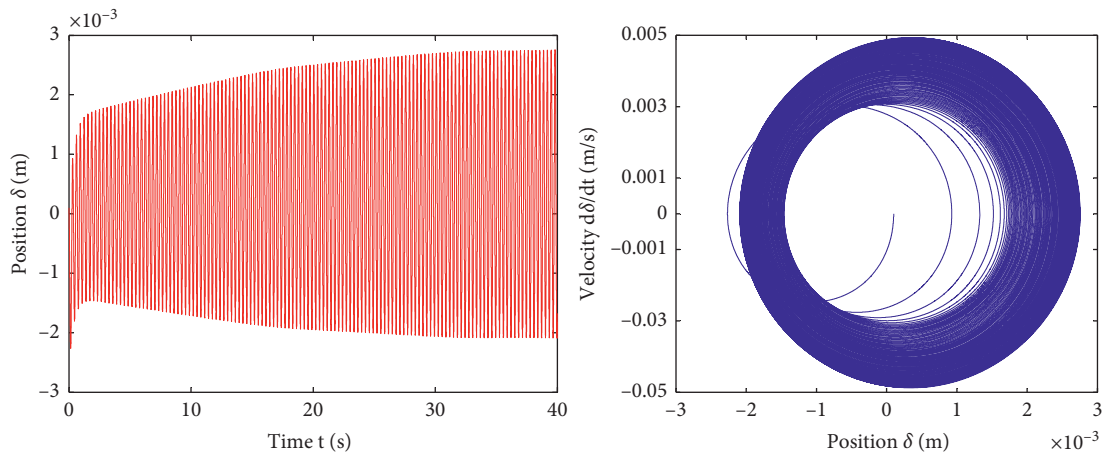


FIGURE 6: The response time domain and phase diagram when $k_p = 1700$.

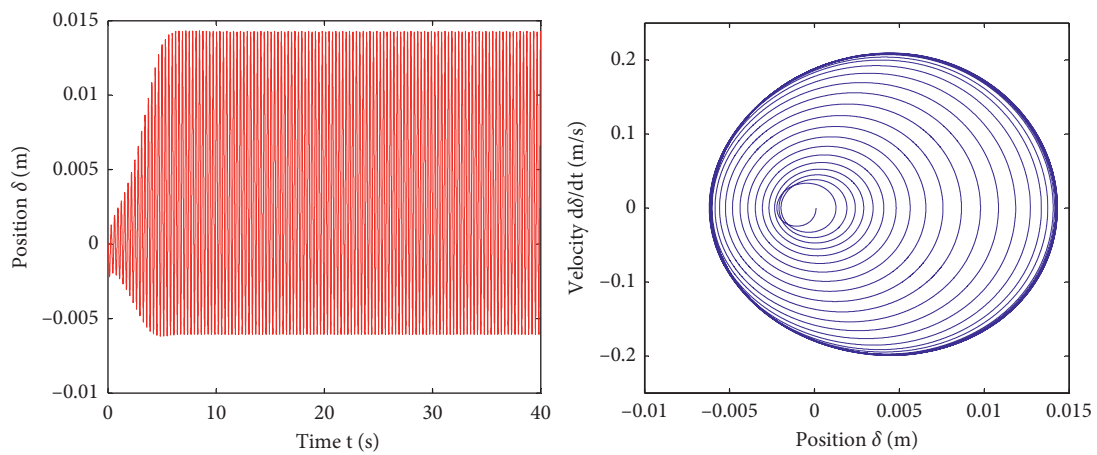


FIGURE 7: The response time domain and phase diagram when $k_p = 1800$.

6. Conclusions

- (1) The dynamics model of the single electromagnet-track beam coupled system of the EMS maglev train is established, with the classical PD control method adopted and the influence of the first-order vibration mode of the track beam taken into consideration.
- (2) It is convenient to determine the stability of the system motion and the Hopf bifurcation, from the composition and symbol of the eigenvalues of the system based on the Hurwitz algebraic criterion instead of solving the specific eigenvalues.
- (3) Take k_p as the bifurcation parameter. When $k_d = 100$, the critical Hopf bifurcation value is calculated as $k_{p_0} = 1690.681$, and it is categorized as supercritical Hopf bifurcation, that is, when $k_p < k_{p_0}$, the system is asymptotically stable, yet Hopf bifurcation occurs as k_p increases gradually beyond k_{p_0} , with the stability of the system lost and a stable limit cycle branched.

Data Availability

The data used to support the findings of this study are included within the article.

Conflicts of Interest

The authors declare that there are no conflicts of interest regarding the publication of this paper.

Acknowledgments

This study was supported by the National Natural Science Foundation of China (grant no. 51875483), National Key R&D Program of China (grant nos. 2016YFB1200601-A03 and 2016YFB1200602-13), and Henan Engineering Research Center of Rail Transit Intelligent Security Open Fund Project 2019 (grant no. 2019KFJJ002).

References

- [1] D. F. Zhou, C. H. Hansen, J. Li et al., "Review of coupled vibration problems in EMS maglev vehicles," *International Journal of Acoustics and Vibration*, vol. 15, no. 1, pp. 10–23, 2010.
- [2] M. Nagai, "The control of magnetic suspension to suppress the self-excited vibration of a flexible guideway," *Transactions of the Japan Society of Mechanical Engineers Series C*, vol. 52, no. 478, pp. 1780–1786, 1986.
- [3] Y. Cai, S. S. Chen, D. M. Rote, and H. T. Coffey, "Vehicle/guideway interaction for high speed vehicles on a flexible guideway," *Journal of Sound and Vibration*, vol. 175, no. 5, pp. 625–646, 1994.
- [4] J.-S. Lee, S.-D. Kwon, M.-Y. Kim, and I. H. Yeo, "A parametric study on the dynamics of urban transit maglev vehicle running on flexible guideway bridges," *Journal of Sound and Vibration*, vol. 328, no. 3, pp. 301–317, 2009.
- [5] K.-J. Kim, J.-B. Han, H.-S. Han, and S.-J. Yang, "Coupled vibration analysis of maglev vehicle-guideway while standing still or moving at low speeds," *Vehicle System Dynamics*, vol. 53, no. 4, pp. 587–601, 2015.
- [6] J.-B. Han, H.-S. Han, S.-S. Kim, S.-J. Yang, and K.-J. Kim, "Design and validation of a slender guideway for maglev vehicle by simulation and experiment," *Vehicle System Dynamics*, vol. 54, no. 3, pp. 370–385, 2016.
- [7] Y. D. Xie and W. S. Chang, "Modelling and simulation of electromagnetic suspension vehicle systems (EMS) in vertical direction," *Journal of the China Railway Society*, vol. 18, no. 4, pp. 47–54, 1996.
- [8] C. F. Zhao and W. M. Zhai, "Maglev vehicle/guideway vertical random response and ride quality," *Vehicle System Dynamics*, vol. 38, no. 3, pp. 185–210, 2002.
- [9] W. H. Ma, R. R. Song, J. Q. Xu, Y. Zang, and S. Luo, "A coupling vibration test bench and the simulation research of a maglev vehicle," *Shock and Vibration*, vol. 2015, Article ID 586910, 14 pages, 2015.
- [10] Y. H. Zhou, J. J. Wu, X. J. Zheng et al., "Analysis of dynamic stability for magnetic levitation vehicles by liapunov characteristic number," *Acta Mechanica Sinica*, vol. 32, no. 1, pp. 42–51, 2000.
- [11] X. H. Shi, L. H. She, and W. S. Chang, "The bifurcation analysis of the EMS maglev vehicle-coupled-guideway system," *Acta Mechanica Sinica*, vol. 36, no. 5, pp. 634–640, 2004.
- [12] H.-P. Wang, J. Li, and K. Zhang, "Stability and hopf bifurcation of the maglev system with delayed speed feedback control," *Acta Automatica Sinica*, vol. 33, no. 8, pp. 829–834, 2007.
- [13] H. Wang, J. Li, and K. Zhang, "Non-resonant response, bifurcation and oscillation suppression of a non-autonomous system with delayed position feedback control," *Nonlinear Dynamics*, vol. 51, no. 3, pp. 447–464, 2008.
- [14] J.-H. Li, J. Li, D.-F. Zhou, and P.-C. Yu, "Self-excited vibration problems of maglev vehicle-bridge interaction system," *Journal of Central South University*, vol. 21, no. 11, pp. 4184–4192, 2014.
- [15] C. F. Zhao and W. M. Zhai, "Dynamic characteristics of electromagnet levitation system," *Journal of Southwest Jiaotong University*, vol. 39, no. 4, pp. 464–468, 2004.
- [16] H. Wang and G. Shen, "Small-scale similarity model of maglev-guideway coupling vibration," *Journal of Traffic and Transportation Engineering*, vol. 14, no. 1, pp. 49–56, 2014.
- [17] H. Wang, X. B. Zhong, and G. Shen, "Levitation control strategy for maglev on elastic track based on kalman filter," *Journal of Central South University*, vol. 45, no. 3, pp. 965–972, 2014.
- [18] L. L. Zhang, L. H. Huang, and Z. Z. Zhang, "Stability and hopf bifurcation of the maglev system with delayed position and speed feedback control," *Nonlinear Dynamics*, vol. 57, no. 1-2, pp. 197–207, 2009.
- [19] L. L. Zhang, Z. Z. Zhang, Z. Q. Long, and A. M. Hao, "Sliding mode control with auto-tuning law for maglev system," *Engineering*, vol. 2, no. 2, pp. 107–112, 2010.
- [20] H. C. Wu and H. R. Fang, "Analysis on stability of suspension control system based on Hurwitz criterion," *Journal of the China Railway Society*, vol. 34, no. 12, pp. 40–45, 2012.
- [21] Y. Sun, J. Xu, H. Qiang, W. Wang, and G. Lin, "Hopf bifurcation analysis of maglev vehicle-guideway interaction vibration system and stability control based on fuzzy adaptive theory," *Computers in Industry*, vol. 108, pp. 197–209, 2019.
- [22] X. Li, D. Wang, D. Liu, L. Xin, and X. Zhang, "Dynamic analysis of the interactions between a low-to-medium-speed maglev train and a bridge: field test results of two typical bridges," *Proceedings of the Institution of Mechanical*

- Engineers, Part F: Journal of Rail and Rapid Transit*, vol. 232, no. 7, pp. 2039–2059, 2018.
- [23] J. Y. Zhang, Y. R. Yang, and J. Zeng, “An algorithm criterion for Hopf bifurcation and its applications in vehicle dynamics,” *Acta Mechanica Sinica*, vol. 32, no. 5, pp. 596–605, 2000.
- [24] B. Hassard, “Bifurcation of periodic solutions of the Hodgkin-Huxley model for the squid giant axon,” *Journal of Theoretical Biology*, vol. 71, no. 3, pp. 401–420, 1978.
- [25] B. Hassard and Y. H. Wan, “Bifurcation formulae derived from center manifold theory,” *Journal of Mathematical Analysis and Applications*, vol. 63, no. 1, pp. 297–312, 1978.